# Fermion Disorder Operator at Gross-Neveu and Deconfined Quantum Criticalities

Zi Hong Liu,[1] Weilun Jiang,[2,3] Bin-Bin Chen,[4] Junchen Rong,[5] Meng Cheng,[6,*] Kai Sun,[7,†] Zi Yang Meng,[4,‡] and Fakher F. Assaad[1,§]

[1]*Institut für Theoretische Physik und Astrophysik and Würzburg-Dresden Cluster of Excellence ct.qmat, Universität Würzburg, 97074 Würzburg, Germany*
[2]*Beijing National Laboratory for Condensed Matter Physics and Institute of Physics, Chinese Academy of Sciences, Beijing 100190, China*
[3]*School of Physical Sciences, University of Chinese Academy of Sciences, Beijing 100190, China*
[4]*Department of Physics and HKU-UCAS Joint Institute of Theoretical and Computational Physics, The University of Hong Kong, Pokfulam Road, Hong Kong SAR, China*
[5]*Institut des Hautes Études Scientifiques, 91440 Bures-sur-Yvette, France*
[6]*Department of Physics, Yale University, New Haven, Connecticut 06520-8120, USA*
[7]*Department of Physics, University of Michigan, Ann Arbor, Michigan 48109, USA*

(Received 11 January 2023; revised 19 April 2023; accepted 8 June 2023; published 28 June 2023)

The fermion disorder operator has been shown to reveal the entanglement information in 1D Luttinger liquids and 2D free and interacting Fermi and non-Fermi liquids emerging at quantum critical points (QCPs) [W. Jiang *et al.*, arXiv:2209.07103]. Here we study, by means of large-scale quantum Monte Carlo simulation, the scaling behavior of the disorder operator in correlated Dirac systems. We first demonstrate the logarithmic scaling behavior of the disorder operator at the Gross-Neveu (GN) chiral Ising and Heisenberg QCPs, where consistent conformal field theory (CFT) content of the GN-QCP in its coefficient is found. Then we study a 2D monopole-free deconfined quantum critical point (DQCP) realized between a quantum-spin Hall insulator and a superconductor. Our data point to negative values of the logarithmic coefficients such that the DQCP does not correspond to a unitary CFT. Density matrix renormalization group calculations of the disorder operator on a 1D DQCP model also detect emergent continuous symmetries.

DOI: 10.1103/PhysRevLett.130.266501

*Introduction and motivation.*—Entanglement witnesses can reveal the fundamental organizing principle of many-body systems. One such witness is the disorder operator [1–4], which hinges on symmetry properties of a system, such as spin rotational invariance or charge conservation. It is an equal-time observable with no need for a replica manifold and is easily accessible to auxiliary field determinantal quantum Monte Carlo (DQMC) simulations [5–7]. For a given system with a U(1) global symmetry, with generator $\hat{Q} = \sum_{i\in V} \hat{n}_i$, the disorder operator carries out a rotation with angle $\theta$ in the entanglement region $M \subset V$, i.e., $X(\theta) = \langle \prod_{i\in M} \exp(i\theta\hat{n}_i)\rangle$, as shown schematically in Figs. 1(d) and 1(e). For states of matter characterized by a finite length scale, such as a band insulator, this rotation only effects the boundary, and generically an area law is expected. For scale invariant systems, logarithmic corrections to the area law reveal critical behavior [8–11]. Furthermore, subleading corrections reflect topological order [12]. In particular, at a (conformal) quantum critical point (QCP), when the boundary of region $M$ is not smooth, the scaling behavior of the disorder operator—similar to that of the entanglement entropy (EE)—acquires a logarithmic corner correction term [13],

$$\ln|X(\theta)| \sim -al + s(\theta)\ln l + c. \tag{1}$$

While the area law coefficient $a$ is sensitive to the UV physics, the log coefficient $s(\theta)$ is universal and reflects the IR physics.

The above has an obvious overlap with the EE and related entanglement spectrum (ES) [13,20–42]. Although in some special cases both the $n$th order Rényi EE, i.e., $-[1/(1-n)]\ln \mathrm{Tr}(\rho_M^n)$, where $\rho_M = \mathrm{Tr}_{\bar{M}}\rho$ is the reduced density matrix, and the disorder operator produce identical results, both quantities differ. Being symmetry based, the disorder operator offers more possibilities such as the detection of emergent symmetries. The aim of this Letter is to investigate these possibilities for Dirac systems.

As mentioned above, the disorder operator and EEs are different quantities, with the former formulated in terms of a global symmetry of the model system and the latter defined without any symmetry considerations. However, their connections from an entanglement perspective can be

 © 2023 American Physical Society

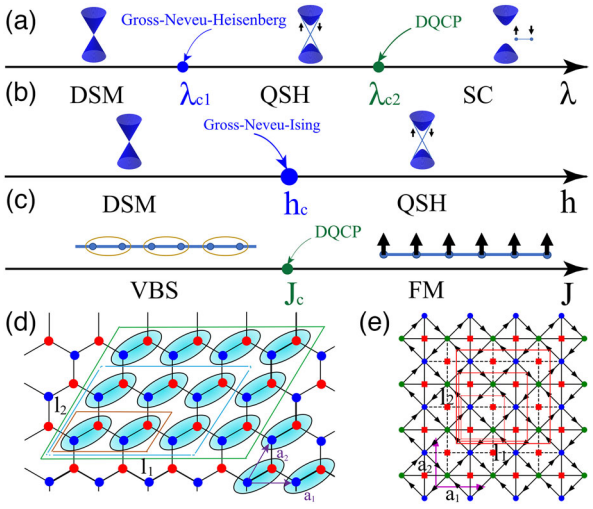


FIG. 1. (a)–(c) Schematic phase diagrams of the 2D DQCP model in Eq. (2), the $\pi$-flux model, and the 1D DQCP model. The 2D DQCP model has three phases: DSM, QSH, and SC, separated by two QCPs: GN-Heisenberg QCP at $\lambda_{c1}$ and DQCP at $\lambda_{c2}$ [14]. For comparison, the $\pi$-flux model also possesses DSM and QSH phases, separated by the GN-Ising QCP at $h_c$ [15–17]. The last one is a 1D model containing VBS and FM phases separated by a DQCP, with $[\mathrm{U}(1)\times\mathrm{U}(1)]\rtimes\mathbb{Z}_2$ emergent symmetry [18,19]. (d),(e) Sketch of parallelogram entanglement region $M$ in the 2D DQCP model and square entanglement region $M$ in the $\pi$-flux model. $\mathbf{a}_1$ and $\mathbf{a}_2$ are unit vectors, and $l_1$ and $l_2$ are the linear lengths of $M$. We define the perimeter $l = 2(l_1 + l_2)$ for both models, which is used to extract the scaling behavior of the disorder operators.

established from two important limits of the disorder operator. The first one is in the small angle limit $\theta \to 0$, where the disorder operator can be mapped to bipartite fluctuations $-\ln|X(\theta)| \propto \theta^2\langle(\sum_{i\in M}(\hat{n}_i - \langle\hat{n}_i\rangle))^2\rangle$ [43]. In the small $\theta$ limit, $s(\theta)$ is proportional to the central charge in the conformal field theory (CFT) critical point [8–11]. The second limit is for noninteracting systems [8,9]. For fermions, the disorder operator at special angles maps onto the Rényi EEs, for example $S_2 = -2\ln|X(\pi/2)|$ and $S_3 = -\ln|X(2\pi/3)|$. The general case can be found in [8] and a similar relation holds for the free scalar theory [9].

Beyond the Gaussian limit, one needs to study the disorder operator with numerical simulations. For boson-spin and topologically ordered systems, it was shown that the log coefficient reflects the CFT content of the QCP [9,10] and the remaining constant reflects the topological degeneracy [12]. Of special importance to this Letter is the disorder operator of the 2D J-Q spin model [44] for the deconfined QCP (DQCP) [45], where the log coefficient at $\theta = \pi$ is negative [11]. This finding, together with the similar negative log coefficient in $S_2$ [36], suggests that the J-Q model realization of the DQCP may not be a unitary CFT (or not a CFT at the first place) [41,46] and calls one to reconsider DQCP related phenomena such as the emergent symmetries [44,47], dangerously irrelevant operators [48,49], weakly first-order transition [50–52], complex fixed points, walking of scaling dimensions [53–55], multicriticalities [56], etc., and the physical mechanism behind them.

Hence, the question arises if the negative log coefficient observed at the J-Q model realization of DQCP is a generic feature or an artifact of the model. Therefore, it is of importance to measure the disorder operator at other 2D DQCP lattice models and also in 1D systems [18,19]. The cleanest one present, without any difficulties or ambiguities of the two length scale [48,49], is the model based on the interacting Dirac fermions [14,57] with emergent SO(5) symmetry from order parameter measurements, as shown in Fig. 1(a) and Eq. (2). It is the focus of this Letter to compute the disorder operator at this DQCP in large-scale DQMC simulations.

*Models and numerical settings.*—We study the model introduced in Ref. [14] with Hamiltonian

$$\hat{H} = -t\sum_{\langle ij\rangle}(\hat{\boldsymbol{c}}_i^\dagger\hat{\boldsymbol{c}}_j + \mathrm{H.c.}) - \lambda\sum_{\hexagon}\left(\sum_{\langle\langle \boldsymbol{ij}\rangle\rangle\in\hexagon}\mathrm{i}\nu_{\boldsymbol{ij}}\hat{\boldsymbol{c}}_{\boldsymbol{i}}^\dagger\boldsymbol{\sigma}\hat{\boldsymbol{c}}_{\boldsymbol{j}} + \mathrm{H.c.}\right)^2, \tag{2}$$

where $\langle\cdots\rangle$ and $\langle\langle\cdots\rangle\rangle$ refer to nearest and next-nearest neighbors on the honeycomb lattice [as shown in Fig. 1(d)]. The phase diagram has been mapped out with DQMC simulations [14,57,58], see Fig. 1(a). As a function of a single parameter $\lambda$ (with $t = 1$ as the energy unit), the phase diagram shows a Gross-Neveu (GN)-Heisenberg QCP at $\lambda_{c1} = 0.0187(2)$ separating a Dirac semimetal (DSM) and a quantum-spin Hall (QSH) insulator, and a DQCP at $\lambda_{c2} = 0.0332(2)$ separating the QSH and $s$-wave superconductor (SC). The key difference between Eq. (2) and the J-Q model is the absence of monopoles. In the J-Q model, the U(1) symmetry is emergent since the lattice breaks it down to $\mathbb{Z}_4$. As a consequence, quadruple monopoles are symmetry allowed, and a second length scale at which the $\mathbb{Z}_4$ symmetry is enhanced to U(1) rotational symmetry obscures the numerical analysis [48]. In the model (2), the U(1) symmetry corresponds to charge conservation present in the microscopic model [we note the same microscopic U(1) symmetry also occurs in a closely related cubic dimer model [59] ]. Although the computational complexity of DQMC for Dirac fermions is much higher than that of the stochastic series expansion QMC [44] for the J-Q model, order parameter calculations support that SU(2) spin and U(1) charge symmetries are enhanced to an emergent SO(5) symmetry at this DQCP. As we shall see below, we still find the nonunitary signature of the DQCP in this model, similar to that of the J-Q model [11,36]. We also find that the logarithmic corrections of disorder operators appear to violate the emergent SO(5) symmetry.

To probe the U(1) charge and the SU(2) spin symmetries, we consider the disorder operators

$$X_c(\theta) = \left\langle\prod_{i\in M}e^{i\hat{n}_i\theta}\right\rangle, \qquad X_s(\theta) = \left\langle\prod_{i\in M}e^{i\hat{m}_i^z\theta}\right\rangle, \tag{3}$$

where $\hat{n}_i = \sum_\sigma \hat{c}^\dagger_{i\sigma}\hat{c}_{i\sigma}$ and $\hat{m}^z_i = \sum_\sigma \sigma \hat{c}^\dagger_{i\sigma}\hat{c}_{i\sigma} = 2\hat{s}^z_i$ are the density and magnetization along the $z$ quantization axis. The operator products $\prod$ are performed in the region $M$ shown in Figs. 1(d) and 1(e). From the definitions in Eq. (3), it easily follows that $X_{c/s}(\theta) = X_{c/s}(\theta + 2\pi)$, and $X_c(\pi) = X_s(\pi)$. A more detailed derivation of the disorder operator is presented in Sec. I of the Supplemental Material [60]. We use the Algorithms for Lattice Fermions(ALF) implementation [61] of the auxiliary field QMC algorithm to study the microscopic model of Eq. (2) and consider linear system sizes $L = 6, 9, 12, 15, 18$ at $\beta = L$.

To further study the GN-QCP and DQCP and for comparisons, we consider two other interacting models. For the GN-QCP, we study Dirac fermions based on the $\pi$-flux square lattice with a fermion-spin coupling model that triggers a GN-Ising QCP toward a QSH phase [15–17]. The phase diagram and the model are shown in Figs. 1(b) and 1(e), respectively. The numerical results are shown in Sec. III in the Supplemental Material [60].

In addition, we consider a 1D DQCP spin model [18,19] with the Hamiltonian written as follows: $\hat{H} = \sum_i (-J_x \hat{S}^x_i \hat{S}^x_{i+1} - J_z \hat{S}^z_i \hat{S}^z_{i+1}) + (K_x \hat{S}^x_i \hat{S}^x_{i+2} + K_z \hat{S}^z_i \hat{S}^z_{i+2})$, which describes a spin chain containing nearest neighbor ferromagnetic interactions $J_x$, $J_z$ and next-nearest neighbor antiferromagnetic interactions $K_x$, $K_z$. The model possesses a discrete $\mathbb{Z}_2^x \times \mathbb{Z}_2^z$ symmetry. We fix $K_x = K_z = 1/2$ and $J_x = 1$, such that the zero temperature phase diagram is described by only one parameter $J_z$, shown in Fig. 1(c). The small and large $J_z$ limits are valence-bond-solid (VBS) and ferromagnetic (FM) phases, separated by a DQCP located at $J_c$. The emergent symmetry here is $[\mathrm{U}(1) \times \mathrm{U}(1)] \rtimes \mathbb{Z}_2$. Previous infinite density matrix renormalization group (DMRG) simulations find $J_c = 1.4645$ [18,19], and we compute the disorder operator with DMRG to verify the presence of emergent continuous symmetry.

*DSM.*—First, we present the results in the DSM phase of the model in Eq. (2). From the measured $|X_c(\theta)|$ and $|X_s(\theta)|$ as a function of the perimeter $l$ (see Sec. II of the Supplemental Material [60]), one can fit the data with the scaling form of Eq. (1) and extract the universal coefficients $s_{c/s}(\theta)$. The results are presented in Figs. 2(a) and 2(b). We note that, when $\lambda = 0$, there is an exact partial particle-hole symmetry $\hat{c}_\uparrow \to \hat{c}_\uparrow, \hat{c}_\downarrow \to \hat{c}^\dagger_\downarrow$, under which $\hat{n}_i \to \hat{m}^z_i$. It is broken explicitly by the interaction term for $\lambda \neq 0$. Nevertheless, since the interaction is irrelevant in the DSM phase, the symmetry is still present in the IR theory (i.e., it is emergent), and therefore we expect that in the IR $s_s(\theta) = s_c(\theta)$ for all values of the angles throughout the entire DSM phase. The result of the size extrapolation $s_{s/c}(\theta)$ is shown in Fig. 2(g). Within our error bars we have $s_s(\theta) = s_c(\theta)$ and compare well with the free case ($\lambda = 0$). It is known at small angle limit $\theta \to 0$, $s_{c/s}(\theta)$ satisfies the quadratic form $s_{c/s}(\theta) = \alpha_{c/s}\theta^2$. The IR CFT gives $\alpha_{c/s} = (AN_\sigma C_{J,\mathrm{free}}/8\pi^2)$, where $N_\sigma = 2$ is the spin flavor,

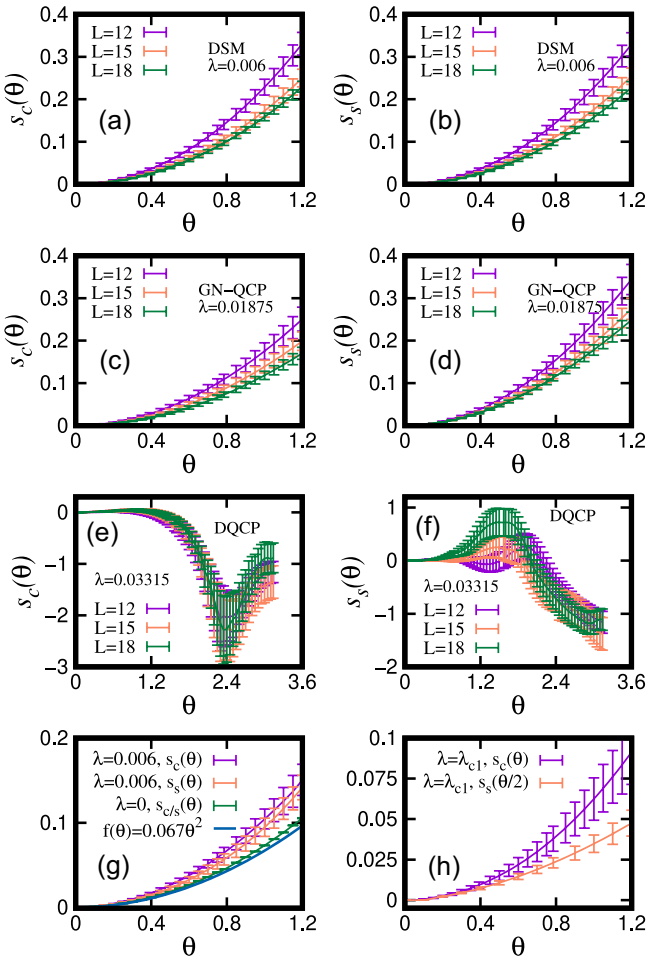


FIG. 2. Logarithmic coefficient $s_{c/s}(\theta)$ in the scaling of the disorder operator as a function of $\theta$ in DSM phase (a),(b); at the GN-QCP at $\lambda_{c1}$ (c),(d); and at the DQCP $\lambda_{c2}$ (e),(f). Different lines represent different system sizes $L$. The logarithmic coefficient $s_{c/s}(\theta)$ extrapolated to the thermodynamic limit are presented at (g) in the DSM phase and (h) at GN-Heisenberg QCP.

and $A \approx 1.30$ is a constant determined by the shape of the region [62] (see the Supplemental Material [60] for more details on $A$). $C_J$ is the current central charge of the CFT. For the DSM phase, we have $C_{J,\mathrm{free}} = 2$ for free Dirac fermions [63]. Extrapolation of $\alpha_{c/s}$ is shown in Fig. 3. We obtain $\alpha_c(\infty) = 0.068(24)$ in Fig. 3(a) and $\alpha_s(\infty) = 0.068(31)$ in Fig. 3(b), fully consistent with the theoretical expectation $\alpha_{c/s} \approx 0.066$.

*QSH and SC.*—The scaling behavior of the disorder operator in the QSH and SC phases is affected by the gapless Goldstone modes originating from continuous symmetry breaking. Our data for $|X_s(\pi/2)|$ and $|X_c(\pi/2)|$ can be found in Sec. II of the Supplemental Material [60]. Given our system size, we find it challenging to distinguish between additive $\ln l$ and multiplicative $l \ln l$ logarithmic corrections. The latter is expected for Goldstone modes as observed in the superfluid phase of the Bose-Hubbard model [10].

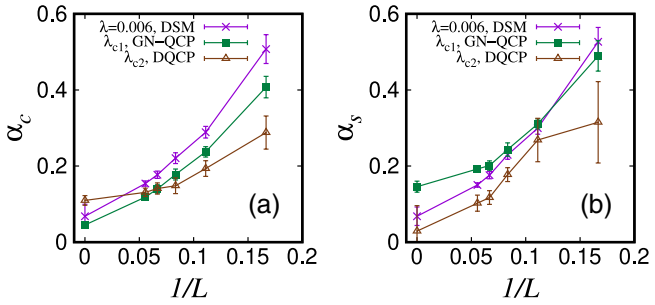


FIG. 3. System-size dependence of $\alpha_{c/s} = s_{c/s}(\theta)/\theta^2$, with $s_{c/s}(\theta)$ obtained from the fitting in Fig. 2. In the DSM phase ($\lambda = 0.006$), extrapolation to the thermodynamic limit $L \to +\infty$ gives $\alpha_{c/s} = 0.06(1)$, consistent with the expected CFT value of $\alpha = (AN_\sigma C_{J,\mathrm{free}}/8\pi^2) \approx 0.066$.

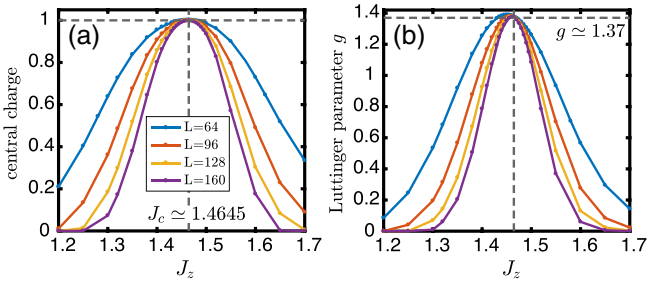


FIG. 4. Emergent symmetry at the 1D DQCP $J_c = 1.4645$. The (a) central charge $c$ and (b) Luttinger parameter $g$ are obtained from the CFT scaling behavior of entanglement entropy $S_{\mathrm{vN}} = (c/3)\ln\tilde{l}$ and disorder operator $-\ln|X_s| = (g/8)\ln\tilde{l}$, with the conformal distance $\tilde{l} = (L/\pi)\sin(\pi l/L)$, which indeed provide the correct values for $c$ and $g$ at the DQCP.

*DQCP.*—There is a body of work suggesting emergent SO(5) symmetry at the DQCP, $\lambda_{c2} = 0.03315$ [49,64], and it is intriguing to study this from the point of view of the disorder operator. To this aim, our model is unusual since the U(1) symmetry is embedded as charge conservation and is present at the UV scale [we note the same microscopic U(1) symmetry also occurs in a closely related cubic dimer model [59] ]. The conjectured emergent SO(5) symmetry at the DQCP implies that the low energy theory is invariant under SO(5) rotations of the superspin vector, consisting of the two components of the superconducting order parameter and the three components of the QSH one [65,66]. Since the charge (spin) disorder operator of Eq. (3) rotates the superconducting (QSH) order parameter by $2\theta$, one expects $s_s(\theta) = s_c(\theta)$ for all values of $\theta$. In the small angle limit, this results in $\alpha_s = \alpha_c$, which stands at odds with our results: $\alpha_c(\infty) = 0.11(1)$ and $\alpha_s = 0.022(63)$, albeit with very large error bars. Furthermore, at larger values of the angle, $s_{s/c}(\theta)$ go negative and differ substantially. Negative values of $s_{c/s}(\theta)$ suggest that the DQCP cannot be described by a unitary CFT, it is a pseudo-critical point. Similar observations were made in the J-Q model, both in the spin disorder operator [11] and entanglement entropy $S_2$ [36].

*GN transitions.*—In contrast to the DQCP $s_{c/s}(\theta)$ at the GN-Heisenberg transition remains positive in finite systems, as shown in Figs. 2(c) and 2(d), and after extrapolation to the thermodynamic limit, shown in Fig. 2(h). This confirms the well-established picture that the GN-Heisenberg transition is described by a unitary CFT. For the GN-Ising transition discussed in Sec. III of the Supplemental Material [60], we find that the central charge $C_J$ is slightly reduced compared with that of the free DSM, consistent with the field-theoretical prediction [67].

At the GN-Heisenberg critical point, partial particle-hole symmetry is not present. This is illustrated by the fact that $s_c(\theta) \neq s_s(\theta)$. Interestingly, our data seem to support the relation $s_c(\theta) \simeq s_s(\theta/2)$.

*1D DQCP.*—As a final example, we study the 1D DQCP model [18,19] of Fig. 1(c) with DMRG simulations. Our aim is to further confirm that disorder operators follow the predictions of the IR theory with emergent continuous symmetries. In Ref. [18], the continuous phase transition between ferromagnetic $z$-FM and VBS phases is determined with high precision. The DQCP point has emergent $[\mathrm{U}(1) \times \mathrm{U}(1)] \rtimes \mathbb{Z}_2$ symmetry with the $x$ FM and $y$ antiferromagnetic constituting the first U(1) and $z$ FM and VBS constituting the second. The Luttinger parameter is determined in previous work at the DQCP from two-point correlation functions to be $g = 1.38(1)$ [18]. Since the lattice model only has discrete symmetries, we compute the spin disorder operator defined as $X_s = \langle \prod_{i \in M} \sigma_i^z \rangle$ (corresponding to $\theta = \pi$) for a region $M$ of length $l$ and extract the scaling behavior from $-\ln(|X_s(l)|) = (g/8)\ln l$, as has been done for the 1D Hubbard model [8,68]. In Fig. 4(a), the central charge $c = 1$ around the DQCP point $J_z \simeq 1.4645$ is extracted from Von Neumann entropy $S_{\mathrm{vN}} = (c/3)\ln\tilde{l}$ with the conformal distance $\tilde{l} = (L/\pi)\sin(\pi l/L)$. In Fig. 4(b), the Luttinger parameter $g \simeq 1.37$ is extracted from the disorder operator on the finite-size systems, following the finite-size scaling form $-\ln(|X_s(l)|) = (g/8)\ln\tilde{l}$. Away from the critical point, and as supported by the data, the log corrections are expected to vanish since all correlation functions are characterized by a finite length scale.

*Discussion.*—The disorder operator is a simple quantity to implement in many numerical approaches. Especially in the realm of DQMC and in comparison to EE and ES, the disorder operator is very easy to access and can be computed "on the fly." Whereas 1D and 2D boson-spin systems, as well as nearly free fermion systems, have been intensively investigated from the point of view of entanglement [13,24–28,35–40,69–79], the simplest interacting fermion lattice models in 2D, that is, Dirac fermions and their interaction-driven GN transitions [14–17,57,80–91] remain challenging. This is mainly because the EE, for example, the $n$th-order Rényi entropy $S_n$, needs to be computed in path-integral QMC simulations with a replicated manifold. Since the typical DQMC simulation for

interacting fermions is already very expensive [usually the computational complexity scales as $O(\beta N^3)$ with $\beta = 1/T$ and $N = L^D$], the construction of the replicated manifold and the ensemble average therein [31,32,34] is challenging. As a result, small system sizes in 2D and often noisy data are insufficient to extract universal scaling properties in EE. We note recent progress in this regard, with better data quality and the approximate $O(\beta N^3)$ scaling [39,41,42].

In contrast, no replica construction is required for the disorder operator. Logarithmic corrections to the area law capture IR physics and provide invaluable insights into critical points. Although it is challenging to control logarithmic corrections to the area law, especially in DQMC, we have presented a large body of data that shows consistent results for Dirac systems. Particularly, we can test for emergent symmetries at the DSM point by comparing particle-hole related disorder operators. One can also extract the central charge $C_J$. Emergent symmetries at a 1D DQCP can equally be tested. The CFT constraint on the sign of the coefficient of the logarithmic correction $s(\theta) > 0$ allows us to test if a putative critical point actually corresponds to a unitary CFT. Using this criterion, we are able to show that our realization of a monopole-free DQCP does not seem to correspond to a unitary CFT. This is consistent with results for the J-Q model [11,36] and hints at the power of the disorder operator. Given the simplicity of computing this quantity, especially within the realm of fermion QMC, many new directions are opened from here, concerning the enigmatic fate of the 2D DQCP theories and their lattice model realizations [41,44,47,50–56,89,90].

W. L. J., B. B. C., and Z. Y. M. acknowledge the support from the Research Grants Council of Hong Kong SAR of China (Projects No. 17301420, No. 17301721, No. AoE/P-701/20, No. 17309822, No. HKU C7037-22G), the ANR/RGC Joint Research Scheme sponsored by Research Grants Council of Hong Kong SAR of China (Project No. A_HKU703/22), the French National Research Agency (Grant No. ANR-22-CE30-0042-01), the Strategic Priority Research Program of the Chinese Academy of Sciences (Grant No. XDB33000000), and the K.C. Wong Education Foundation (Grant No. GJTD-2020-01). F. F. A. and Z. H. L. acknowledge financial support from the DFG through the Würzburg-Dresden Cluster of Excellence on Complexity and Topology in Quantum Matter—*ct.qmat* (EXC 2147, Project No. 390858490), as well as the SFB 1170 on Topological and Correlated Electronics at Surfaces and Interfaces (Project No. 258499086). We thank the HPC2021 platform under the Information Technology Services at the University of Hong Kong and the Tianhe-II platform at the National Supercomputer Center in Guangzhou for their technical support and generous allocation of CPU time. We equally gratefully acknowledge the Gauss Centre for Supercomputing e.V. for funding this project by providing computing time on the GCS Supercomputer SuperMUC-NG at Leibniz Supercomputing Centre.

*m.cheng@yale.edu
†sunkai@umich.edu
‡zymeng@hku.hk
§fakher.assaad@physik.uni-wuerzburg.de

[1] L. P. Kadanoff and H. Ceva, Phys. Rev. B **3**, 3918 (1971).
[2] E. Fradkin, J. Stat. Phys. **167**, 427 (2017).
[3] Z. Nussinov and G. Ortiz, Proc. Natl. Acad. Sci. U.S.A. **106**, 16944 (2009).
[4] Z. Nussinov and G. Ortiz, Ann. Phys. (Amsterdam) **324**, 977 (2009).
[5] R. Blankenbecler, D. J. Scalapino, and R. L. Sugar, Phys. Rev. D **24**, 2278 (1981).
[6] S. R. White, D. J. Scalapino, R. L. Sugar, E. Y. Loh, J. E. Gubernatis, and R. T. Scalettar, Phys. Rev. B **40**, 506 (1989).
[7] F. Assaad and H. Evertz, in *Computational Many-Particle Physics*, Lecture Notes in Physics Vol. 739, edited by H. Fehske, R. Schneider, and A. Weiße (Springer, Berlin, Heidelberg, 2008), pp. 277–356.
[8] W. Jiang, B.-B. Chen, Z. H. Liu, J. Rong, F. F. Assaad, M. Cheng, K. Sun, and Z. Y. Meng, arXiv:2209.07103.
[9] J. Zhao, Z. Yan, M. Cheng, and Z. Y. Meng, Phys. Rev. Res. **3**, 033024 (2021).
[10] Y.-C. Wang, M. Cheng, and Z. Y. Meng, Phys. Rev. B **104**, L081109 (2021).
[11] Y.-C. Wang, N. Ma, M. Cheng, and Z. Y. Meng, SciPost Phys. **13**, 123 (2022).
[12] B.-B. Chen, H.-H. Tu, Z. Y. Meng, and M. Cheng, Phys. Rev. B **106**, 094415 (2022).
[13] E. Fradkin and J. E. Moore, Phys. Rev. Lett. **97**, 050404 (2006).
[14] Y. Liu, Z. Wang, T. Sato, M. Hohenadler, C. Wang, W. Guo, and F. F. Assaad, Nat. Commun. **10**, 1 (2019).
[15] Y.-Y. He, X. Y. Xu, K. Sun, F. F. Assaad, Z. Y. Meng, and Z.-Y. Lu, Phys. Rev. B **97**, 081110(R) (2018).
[16] Y. Liu, W. Wang, K. Sun, and Z. Y. Meng, Phys. Rev. B **101**, 064308 (2020).
[17] T.-T. Wang and Z. Y. Meng, arXiv:2304.00034.
[18] R.-Z. Huang, D.-C. Lu, Y.-Z. You, Z. Y. Meng, and T. Xiang, Phys. Rev. B **100**, 125137 (2019).
[19] B. Roberts, S. Jiang, and O. I. Motrunich, Phys. Rev. B **99**, 165143 (2019).
[20] J. L. Cardy and I. Peschel, Nucl. Phys. **B300**, 377 (1988).
[21] M. Srednicki, Phys. Rev. Lett. **71**, 666 (1993).
[22] C. Holzhey, F. Larsen, and F. Wilczek, Nucl. Phys. **B424**, 443 (1994).
[23] P. Calabrese and J. Cardy, J. Stat. Mech. (2004) P06002.
[24] H. Casini and M. Huerta, Nucl. Phys. **B764**, 183 (2007).
[25] A. Kitaev and J. Preskill, Phys. Rev. Lett. **96**, 110404 (2006).
[26] M. Levin and X.-G. Wen, Phys. Rev. Lett. **96**, 110405 (2006).
[27] H. Li and F. D. M. Haldane, Phys. Rev. Lett. **101**, 010504 (2008).
[28] D. Poilblanc, Phys. Rev. Lett. **105**, 077202 (2010).
[29] H. F. Song, S. Rachel, C. Flindt, I. Klich, N. Laflorencie, and K. Le Hur, Phys. Rev. B **85**, 035409 (2012).
[30] T. Grover, Phys. Rev. Lett. **111**, 130402 (2013).
[31] F. F. Assaad, T. C. Lang, and F. Parisen Toldin, Phys. Rev. B **89**, 125121 (2014).
[32] F. F. Assaad, Phys. Rev. B **91**, 125146 (2015).

[33] N. Laflorencie, Phys. Rep. **646**, 1 (2016).
[34] F. Parisen Toldin and F. F. Assaad, Phys. Rev. Lett. **121**, 200602 (2018).
[35] J. D'Emidio, Phys. Rev. Lett. **124**, 110602 (2020).
[36] J. Zhao, Y.-C. Wang, Z. Yan, M. Cheng, and Z. Y. Meng, Phys. Rev. Lett. **128**, 010601 (2022).
[37] Z. Yan and Z. Y. Meng, Nat. Commun. **14**, 2360 (2023).
[38] J. Zhao, B.-B. Chen, Y.-C. Wang, Z. Yan, M. Cheng, and Z. Y. Meng, npj Quantum Mater. **7**, 69 (2022).
[39] J. D'Emidio, R. Orus, N. Laflorencie, and F. de Juan, arXiv:2211.04334.
[40] M. Song, J. Zhao, Z. Yan, and Z. Y. Meng, arXiv:2210.10062.
[41] Y. Da Liao, G. Pan, W. Jiang, Y. Qi, and Z. Y. Meng, arXiv:2302.11742.
[42] G. Pan, Y. Da Liao, W. Jiang, J. D'Emidio, Y. Qi, and Z. Y. Meng, arXiv:2303.14326.
[43] H. F. Song, S. Rachel, C. Flindt, I. Klich, N. Laflorencie, and K. Le Hur, Phys. Rev. B **85**, 035409 (2012).
[44] A. W. Sandvik, Phys. Rev. Lett. **98**, 227202 (2007).
[45] T. Senthil, L. Balents, S. Sachdev, A. Vishwanath, and M. P. A. Fisher, Phys. Rev. B **70**, 144407 (2004).
[46] H. Casini and M. Huerta, J. High Energy Phys. 11 (2012) 087.
[47] N. Ma, Y.-Z. You, and Z. Y. Meng, Phys. Rev. Lett. **122**, 175701 (2019).
[48] H. Shao, W. Guo, and A. W. Sandvik, Science **352**, 213 (2016).
[49] A. Nahum, J. T. Chalker, P. Serna, M. Ortuño, and A. M. Somoza, Phys. Rev. X **5**, 041048 (2015).
[50] A. B. Kuklov, M. Matsumoto, N. V. Prokof'ev, B. V. Svistunov, and M. Troyer, Phys. Rev. Lett. **101**, 050405 (2008).
[51] K. Chen, Y. Huang, Y. Deng, A. B. Kuklov, N. V. Prokof'ev, and B. V. Svistunov, Phys. Rev. Lett. **110**, 185701 (2013).
[52] J. D'Emidio, A. A. Eberharter, and A. M. Läuchli, arXiv:2106.15462.
[53] A. Nahum, Phys. Rev. B **102**, 201116(R) (2020).
[54] R. Ma and C. Wang, Phys. Rev. B **102**, 020407(R) (2020).
[55] V. Gorbenko, S. Rychkov, and B. Zan, J. High Energy Phys. 10 (2018) 108.
[56] B. Zhao, J. Takahashi, and A. W. Sandvik, Phys. Rev. Lett. **125**, 257204 (2020).
[57] Y. Liu, Z. Wang, T. Sato, W. Guo, and F. F. Assaad, Phys. Rev. B **104**, 035107 (2021).
[58] M. Bercx, F. Goth, J. S. Hofmann, and F. F. Assaad, SciPost Phys. **3**, 013 (2017).
[59] G. J. Sreejith, S. Powell, and A. Nahum, Phys. Rev. Lett. **122**, 080601 (2019).
[60] See Supplemental Material at http://link.aps.org/supplemental/10.1103/PhysRevLett.130.266501, for details of QMC simulation, the original data, and related theoretical analysis to coordinate with the results in the main text. The Supplemental Material is organized in four sections: in Sec. I, we provide the details of the QMC simulation and properties on the disorder operator. In Secs. II–IV, we will discuss the results of the 2D DQCP model, 2D $\pi$-flux model, and 1D DQCP model in sequence.
[61] F. F. Assaad, M. Bercx, F. Goth, A. Götz, J. S. Hofmann, E. Huffman, Z. Liu, F. P. Toldin, J. S. E. Portela, and J. Schwab, SciPost Phys. Codebases 1 (2022), 10.21468/SciPostPhysCodeb.1.
[62] X.-C. Wu, C.-M. Jian, and C. Xu, SciPost Phys. **11**, 33 (2021).
[63] J. Helmes, L. E. Hayward Sierens, A. Chandran, W. Witczak-Krempa, and R. G. Melko, Phys. Rev. B **94**, 125142 (2016).
[64] A. Nahum, P. Serna, J. T. Chalker, M. Ortuño, and A. M. Somoza, Phys. Rev. Lett. **115**, 267203 (2015).
[65] A. Tanaka and X. Hu, Phys. Rev. Lett. **95**, 036402 (2005).
[66] T. Senthil and M. P. A. Fisher, Phys. Rev. B **74**, 064405 (2006).
[67] L. Iliesiu, F. Kos, D. Poland, S. S. Pufu, and D. Simmons-Duffin, J. High Energy Phys. 01 (2018) 036.
[68] In our DMRG calculations, we take the periodic boundary condition and confirm the data (including von Neumann EE and disorder operator) are well converged with up to $D = 1024$ bond states kept in the simulations.
[69] J. Helmes and S. Wessel, Phys. Rev. B **89**, 245120 (2014).
[70] G. Vidal, J. I. Latorre, E. Rico, and A. Kitaev, Phys. Rev. Lett. **90**, 227902 (2003).
[71] M. B. Hastings, I. González, A. B. Kallin, and R. G. Melko, Phys. Rev. Lett. **104**, 157201 (2010).
[72] F. Pollmann, A. M. Turner, E. Berg, and M. Oshikawa, Phys. Rev. B **81**, 064439 (2010).
[73] L. Fidkowski, Phys. Rev. Lett. **104**, 130502 (2010).
[74] S. Humeniuk and T. Roscilde, Phys. Rev. B **86**, 235116 (2012).
[75] S. Inglis and R. G. Melko, Phys. Rev. E **87**, 013306 (2013).
[76] D. J. Luitz, X. Plat, N. Laflorencie, and F. Alet, Phys. Rev. B **90**, 125105 (2014).
[77] S. Inglis and R. G. Melko, New J. Phys. **15**, 073048 (2013).
[78] A. B. Kallin, E. M. Stoudenmire, P. Fendley, R. R. P. Singh, and R. G. Melko, J. Stat. Mech. (2014) 06009.
[79] A. B. Kallin, K. Hyatt, R. R. P. Singh, and R. G. Melko, Phys. Rev. Lett. **110**, 135702 (2013).
[80] S. Chandrasekharan and A. Li, Phys. Rev. D **88**, 021701(R) (2013).
[81] Y. Otsuka, S. Yunoki, and S. Sorella, Phys. Rev. X **6**, 011029 (2016).
[82] N. Zerf, L. N. Mihaila, P. Marquard, I. F. Herbut, and M. M. Scherer, Phys. Rev. D **96**, 096010 (2017).
[83] B. Ihrig, L. N. Mihaila, and M. M. Scherer, Phys. Rev. B **98**, 125109 (2018).
[84] T. C. Lang and A. M. Läuchli, Phys. Rev. Lett. **123**, 137602 (2019).
[85] M. Schuler, S. Hesselmann, S. Whitsitt, T. C. Lang, S. Wessel, and A. M. Läuchli, Phys. Rev. B **103**, 125128 (2021).
[86] S. M. Tabatabaei, A.-R. Negari, J. Maciejko, and A. Vaezi, Phys. Rev. Lett. **128**, 225701 (2022).
[87] Z. H. Liu, M. Vojta, F. F. Assaad, and L. Janssen, Phys. Rev. Lett. **128**, 087201 (2022).

[88] R. S. Erramilli, L. V. Iliesiu, P. Kravchuk, A. Liu, D. Poland, and D. Simmons-Duffin, J. High Energy Phys. 02 (2023) 036.
[89] Y. D. Liao, X. Y. Xu, Z. Y. Meng, and Y. Qi, Phys. Rev. B **106**, 075111 (2022).
[90] Y. D. Liao, X. Y. Xu, Z. Y. Meng, and Y. Qi, Phys. Rev. B **106**, 115149 (2022).
[91] Y. D. Liao, X. Y. Xu, Z. Y. Meng, and Y. Qi, Phys. Rev. B **106**, 155159 (2022).